J|A|C|S
ARTICLES
Published on Web 03/22/2006

Unprecedented Alkene Complex of Zinc(II): Structures and Bonding of Divinylzinc Complexes

Alfred Wooten, Patrick J. Carroll, Aaron G. Maestri, and Patrick J. Walsh*

Contribution from the P. Roy and Diana T. Vagelos Laboratories, Department of Chemistry, University of Pennsylvania, 231 South 34th Street, Philadelphia, Pennsylvania 19104-6323

Received January 3, 2006; E-mail: pwalsh@sas.upenn.edu

Abstract: This report describes the solid-state structures of a series of divinylzinc complexes, one of which represents the only structurally characterized zinc(II) π-complex. Vinylzinc reagents, $Zn[C(Me)=CH_2]_2$ (**1**) and $Zn[C(H)=CMe_2]_2$ (**2**), have been synthesized and isolated as white crystalline solids in 66 and 72% yield, respectively. Each compound exhibits an infinite polymeric architecture in the solid state via a series of zinc-π (**1**) and zinc-σ-bonded (**2**) bridging interactions. Addition of chelating ligands to these divinylzinc compounds allowed isolation of the monomeric adducts (bipy)$Zn[C(Me)=CH_2]_2$ (**1•bipy**), (tmeda)$Zn[C(Me)=CH_2]_2$ (**1•tmeda**), (bipy)$Zn[C(H)=CMe_2]_2$ (**2•bipy**), and (tmeda)$Zn[C(H)=CMe_2]_2$ (**2•tmeda**), of which **1•bipy**, **2•bipy**, and **2•tmeda** have been characterized crystallographically.

Introduction

Since the formation of a platinum ethylene complex by Zeise, compounds containing coordinated olefins have been isolated for numerous metals.[1] In many cases, these complexes are quite stable and the olefin is found to behave as a spectator ligand during reactions at the metal center. In other systems, however, olefin binding is weak and the coordinated olefin is very reactive with a transient existence. The stability of metal−olefin complexes can be qualitatively explained by the synergistic interaction of σ-donation from the olefin π-orbital to the metal and π-back-bonding from a filled metal d-orbital into the π^*-orbital of the olefin.[1−4] It has been suggested that the accepting ability of a metal correlates with its electron affinity and that π-donation is related to the promotion energy.[5,6] Metals with high electron affinity, therefore, readily accept electron density from the olefin π-orbital, while metals with low promotional energy actively donate electron density to the olefin π^*-orbital.

In recent years, the search for new olefin and alkyne complexes has focused on d^0 metal centers.[7−29] Olefin complexes of d^0 transition metals are proposed to be reactive intermediates in olefin polymerization reactions.[30−41] Such intermediates are destabilized by the absence of conventional metal-π^*-back-bonding. To increase the binding of olefins to d^0 metal complexes, initial efforts focused on the use of ligands with pendent vinyl groups to exploit the chelation effect. This approach has proven successful with main group,[42−44]

(1) Crabtree, R. H. *The Organometallic Chemistry of the Transition Metals*, 3 ed.; John Wiley and Sons: New York, 2001.
(2) Dewar, M. J. S. *Bull. Soc. Chim. Fr.* **1951**, *18*, C71−C79.
(3) Chatt, J.; Duncanson, L. A. *J. Chem. Soc.* **1953**, 2939−2347.
(4) Frenking, G. In *Modern Coordination Chemistry*; Leigh, G. J., Winterton, N., Eds.; Royal Society of Chemistry: Cambridge, 2002; pp 111−122.
(5) Nyholm, R. S. *Proc. Chem. Soc.* **1961**, 273−296.
(6) Elschenbroich, C.; Salzer, A. *Organometallics: A Concise Introduction*, 2 ed.; VCH Publishers Inc.: New York, 1992.
(7) Burns, C. J.; Andersen, R. A. *J. Am. Chem. Soc.* **1987**, *109*, 915−917.
(8) Nolan, S. P.; Marks, T. J. *J. Am. Chem. Soc.* **1989**, *111*, 8538−8540.
(9) Kress, J.; Osborn, J. A. *Angew. Chem., Int. Ed. Engl.* **1992**, *31*, 1585−1587.
(10) Ballard, D. G. H.; Burnham, D. R.; Twose, D. L. *J. Catal.* **1976**, *44*, 116−125.
(11) Williams, R. A.; Hanusa, T. P.; Huffman, J. C. *J. Am. Chem. Soc.* **1990**, *112*, 2454−2455.
(12) Troyanov, S. I.; Varga, V.; Mach, K. *Organometallics* **1993**, *12*, 2820−2824.
(13) Evans, W. J.; Perotti, J. M.; Brady, J. C.; Ziller, J. W. *J. Am. Chem. Soc.* **2003**, *125*, 5204−5212.
(14) Casey, C. P.; Hallenbeck, S. L.; Pollock, D. W.; Landis, C. R. *J. Am. Chem. Soc.* **1995**, *117*, 9770−9771.
(15) Casey, C. P.; Hallenbeck, S. L.; Wright, J. M.; Landis, C. R. *J. Am. Chem. Soc.* **1997**, *119*, 9680−9690.
(16) Casey, C. P.; Fagan, M. A.; Hallenbeck, S. L. *Organometallics* **1998**, *17*, 287−289.
(17) Casey, C. P.; Carpenetti, D. W. I.; Sakurai, H. *J. Am. Chem. Soc.* **1999**, *121*, 9483−9484.
(18) Casey, C. P.; Klein, J. F.; Fagan, M. A. *J. Am. Chem. Soc.* **2000**, *122*, 4320−4330.
(19) Casey, C. P.; Carpenetti, D. W. *Organometallics* **2000**, *19*, 3970−3977.
(20) Casey, C. P.; Singer, S. W.; Powell, D. R.; Hayashi, R. K.; Kavana, M. *J. Am. Chem. Soc.* **2001**, *123*, 1090−1100.
(21) Casey, C. P.; Lee, T. Y.; Tunge, J. A.; Carpenetti, D. W. *J. Am. Chem. Soc.* **2001**, *123*, 10762−10763.
(22) Humphries, M. J.; Douthwaite, R. E.; Green, M. L. H. *J. Chem. Soc., Dalton Trans.* **2000**, 2952−2959.
(23) Witte, P. T.; Meetsma, A.; Hessen, B.; Budzelaar, P. H. M. *J. Am. Chem. Soc.* **1997**, *119*, 10561−10562.
(24) Karl, J.; Dahlmann, M.; Erker, G.; Bergander, K. *J. Am. Chem. Soc.* **1998**, *120*, 5643−5652.
(25) Galakhov, M. V.; Heinz, G.; Royo, P. *Chem. Commun.* **1998**, 17−18.
(26) Wu, Z.; Jordan, R. F.; Petersen, J. L. *J. Am. Chem. Soc.* **1995**, *117*, 5867−5868.
(27) Casey, C. P.; Tunge, J. A.; Lee, T. Y.; Carpenetti, D. W. *Organometallics* **2002**, *21*, 389−396.
(28) Horton, A. D.; Orpen, A. G. *Organometallics* **1992**, *11*, 8−10.
(29) Stoebenau, E. J.; Jordan, R. F. *J. Am. Chem. Soc* **2004**, *126*, 11170−11171.
(30) Gladysz, J. *Chem. Rev.* **2000**, *100*, 1167−1168.
(31) Bochmann, M. *J. Chem. Soc., Dalton Trans.* **1996**, 255−270.
(32) Boffa, L. S.; Novak, B. M. *Chem. Rev.* **2000**, *100*, 1479−1493.
(33) Arlman, E. J.; Cossee, P. *J. Catal.* **1964**, *3*, 99−104.
(34) Brookhart, M.; Green, M. L. H.; Wong, L.-L. *Prog. Inorg. Chem.* **1988**, *36*, 1−124.
(35) Brintzinger, H. H.; Fischer, D.; Malhaupt, R.; Rieger, B.; Waymouth, R. M. *Angew. Chem., Int. Ed. Engl.* **1995**, *34*, 1143−1170.
(36) Gibson, V. C.; Spitzmesser, S. K. *Chem. Rev.* **2003**, *103*, 283−315.
(37) Jordan, R. F. *J. Mol. Catal. A: Chem.* **1998**, *128*, 337.
(38) Kaminsky, W.; Arndt, M. *Adv. Polym. Sci* **1997**, *127*, 143−187.
(39) Macchioni, A. *Chem. Rev.* **2005**, *105*, 2039−2073.
(40) McKnight, A. L.; Waymouth, R. M. *Chem. Rev.* **1998**, *98*, 2587−2598.
(41) Pedeutour, J. N.; Radhakrishnan, K.; Cramail, H.; Deffieux, A. *Macromol. Rapid Commun.* **2001**, *22*, 1095−1123.

10.1021/ja058700x CCC: $33.50

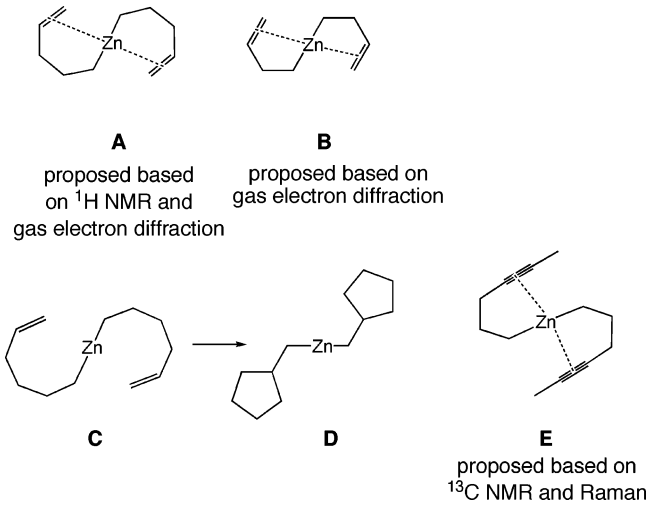

Figure 1. Proposed interaction between dialkylzinc compounds bearing pendent unsaturated groups.

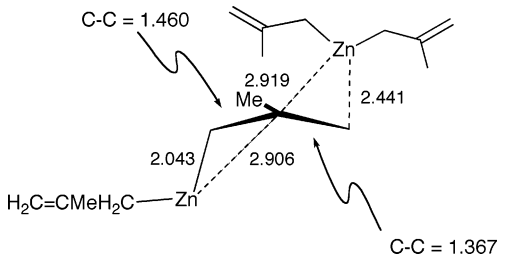

Figure 2. Drawing of the interaction of one methallyl group with two zinc centers in (2-methylallyl)$_2$Zn. Bond lengths are in Å.

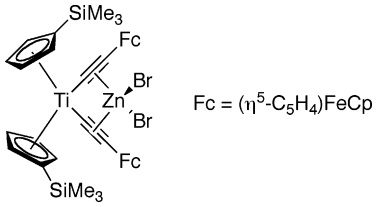

Figure 3.

transition,[14−19,24−26] and lanthanide[13] metal complexes lacking d-electrons available for back-bonding. In some cases, convincing NMR spectroscopic evidence has been reported, while in others, compounds were sufficiently crystalline for X-ray structure determination.[11,13,26,44]

On the basis of the Dewar−Chatt−Duncanson model, it is easy to understand why olefin complexes of d^0 metals are more labile than olefin complexes of metals with d-electrons. Less obvious, however, is the reason for the scarcity of olefin complexes with certain d^{10} metals. While d^{10} nickel, palladium, and platinum complexes readily form stable adducts with olefins, d^{10} complexes of zinc, cadmium, and mercury do not. Examination of the electron affinity and promotion energy for these metals provides insight into this observation. Nickel(0), palladium(0), and platinum(0) have low promotion energies (1.7−4.23 eV) and are, therefore, strong π-back-bonders. In contrast, zinc(II) and cadmium(II) have very high promotional energies (17.1 and 16.6 eV, respectively), while that of mercury(II) is lower (12.8 eV).[6] On the basis of the high promotional energy, olefin complexes of zinc are predicted to be rare, a fact confirmed by the lack of such structures in the Cambridge Crystallographic Data Centre.

Experimental support for solution Zn···C interactions is also sparse. Early NMR studies of diorganozinc compounds with pendent carbon−carbon double and triple bonds provide the first hints of zinc−olefin interactions. Small shifts in the vinyl region of the ^{1}H NMR spectra between 1-pentene and di(pent-4-enyl)-zinc were interpreted as a Zn···alkene interaction (**A**, Figure 1).[45−47] Alternatively, no shifts were observed in the ^{1}H NMR spectra of di(but-3-enyl)zinc (**B**) or di(hex-5-enyl)zinc (**C**). The latter, however, slowly undergoes cyclization (Figure 1), which presumably involves an intermediate with a Zn−π-interaction.[48] Haaland and co-workers examined the molecular structure of di(pent-4-enyl)zinc (**A**) and di(but-3-enyl)zinc (**B**) by gas electron diffraction and found evidence for a weak intramolecular interaction between the zinc and the carbon−carbon double bonds. On the basis of these data, the Zn···C distances were estimated to be between 3.00 and 3.15 Å.[49] These distances are considerably longer than typical Zn−C bonds in a dialkylzinc compound (1.9−2.1 Å) and significantly longer than would be predicted for zinc olefin complexes. Similarly, examination of di(hex-4-ynyl)zinc (**E**) by ^{1}H and ^{13}C{^{1}H} NMR and Raman spectroscopy suggested the presence of an intramolecular interaction between the zinc center and the carbon−carbon triple bond (Figure 1). Increasing the number of methylene groups in the tether by one to di(hept-5-ynyl)zinc gave no indication of chelation of the pendent alkyne.[50,51]

The interaction of zinc(II) with charged conjugated π-systems, such as cyclopentadienyl and allyl groups, is common.[52−56] These Zn−C π-interactions are special cases because the negative charge of the ligand is delocalized over the π-system and coulombic interactions play a significant role in metal−ligand attractive interactions. Benn and co-workers[56] examined the structures of a series of zinc allyl derivatives by solid-state ^{13}C NMR spectroscopy. Both (allyl)$_2$Zn and (2-methylallyl)-ZnCl were concluded to exhibit η^3-bonding to zinc in the solid state. In the case of (2-methylallyl)$_2$Zn, the solid-state structure consists of allyls that bind to one zinc in an η^1-fashion (Zn−C = 2.043(1) Å, Figure 2). The terminal carbon of the allyl interacts with a neighboring zinc with a distance of 2.441(1) Å, and both these zinc atoms are located slightly over 2.90 Å from the central carbon of the allyl. The C−C distances in the allyl are 1.367(1) and 1.460(1) Å. A drawing of this interaction that shows distances to one allyl is illustrated in Figure 2. The unsymmetric bonding in this structure is clearly different than

(42) Hata, G. *Chem. Commun.* **1968**, 7−9.
(43) Dolzine, T. W.; Oliver, J. P. *J. Am. Chem. Soc.* **1974**, *96*, 1737−1740.
(44) Schumann, H.; Schutte, S.; Kroth, H.-J.; Lentz, D. *Angew. Chem., Int. Ed.* **2004**, *43*, 6208−6211.
(45) St. Denis, J.; Oliver, J. P. *J. Organomet. Chem.* **1972**, *44*, C32−C36.
(46) St. Denis, J.; Oliver, J. P. *J. Organomet. Chem.* **1974**, *71*, 315−323.
(47) Albright, M. J.; St. Denis, J. N.; Oliver, J. P. *J. Organomet. Chem.* **1977**, *125*, 1−8.
(48) Denis, J.; Oliver, J. P. *J. Organomet. Chem.* **1974**, *71*, 315−323.
(49) Haaland, A.; Lehmkuhl, H.; Nehl, H. *Acta Chem. Scand.* **1984**, *A38*, 547−553.
(50) Okninska, E.; Starowieyski, K. B. *J. Organomet. Chem.* **1988**, *347*, 1−3.
(51) Okninska, E.; Starowieyski, K. B. *J. Organomet. Chem.* **1989**, *376*, 7−13.
(52) Haaland, A.; Samdal, S.; Seip, R. *J. Organomet. Chem.* **1978**, *153*, 187−192.
(53) Budzelaar, P. H. M.; Boersma, J.; Kerk, G. J. M. V. D. *J. Organomet. Chem.* **1985**, *281*, 123−130.
(54) Blom, R.; Boersma, J.; Budzelaar, P. H. M.; Fisher, B.; Haaland, A.; Volden, H. V.; Weidlein, J. *Acta Chem. Scand. A* **1986**, *40*, 113−120.
(55) Blom, R.; Haaland, A.; Weidlein, J. *J. Chem. Soc., Chem. Commun.* **1985**, 266−267.
(56) Benn, R.; Grondey, H.; Lehmkuhl, H.; Nehl, H.; Angermund, K.; Kruger, C. *Angew. Chem., Int. Ed. Engl.* **1987**, *26*, 1279−1280.

Scheme 1. Proposed Stereodirecting Effect in the Allylzincation Reaction

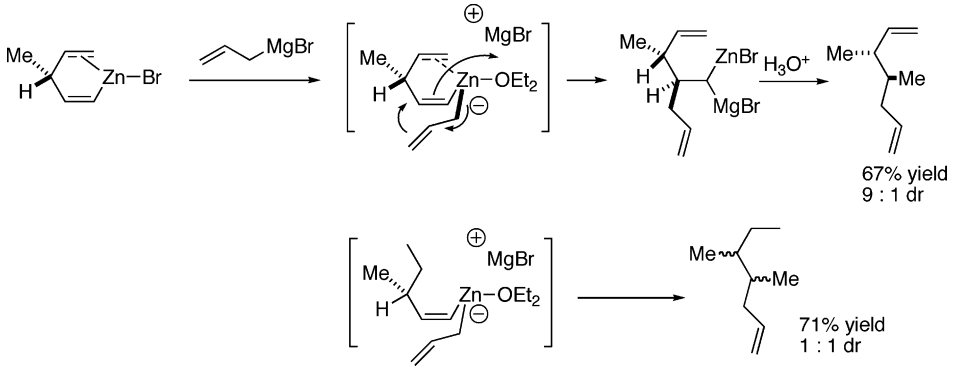

what would be expected for a zinc−olefin complex of ethylene or propylene.

In addition, examples of heterodinuclear complexes with zinc−alkyne π-bonds have been reported by Lang and co-workers.[57] Employing the tweezer-like bis(acetylide) host, (η^5-C_5H_4−$SiMe_3)_2Ti(CCR)_2$, complexes of $ZnCl_2$ and $ZnBr_2$ were isolated, and the structure was determined for the $ZnBr_2$ derivative (Figure 3). Due to the geometrical constraints of the titanium bis(acetylide) complexes, the zinc bonds with the titanium acetylide α-carbons with distances of 2.181(5) and 2.217(5) Å and to the β-carbons with distances of 2.393(5) and 2.703(5) Å.[57]

Despite limited experimental support for zinc−olefin complexes, the interaction of zinc(II) with π-systems has been proposed to explain the acyclic stereocontrol in various reactions.[58,59] One such example is the allylzincation reaction shown in Scheme 1.[58,59] The high degree of acyclic stereocontrol observed was explained by coordination of the pendent olefin to zinc. It was proposed that the allyl group is diastereoselectively delivered to the intermediate metallocycle anti to the methyl group. Rearrangement gave the organobimetallic intermediate[60] that was protonated to furnish the observed diene with high diastereomeric ratio (dr, 9:1). In contrast, when an ethyl group was substituted for the vinyl group, the reaction proceeded with no diastereoselectivity (Scheme 1).

To probe the interaction of zinc(II) with C=C bonds, we have undertaken a structural study of divinylzinc complexes, which led to the discovery of an unprecedented zinc−olefin complex. This structure lends credence to the proposed intermediacy of zinc−olefin interactions in reactions of organozinc complexes.

Results and Discussion

Synthesis of $Zn[C(Me)=CH_2]_2$ and Derivatives. In connection with our interests in the synthesis of enantioenriched epoxy alcohols,[61,62] we required the use of a variety of divinylzinc reagents. Luche and co-workers previously described the synthesis of divinylzinc compounds utilizing ultrasound and ethereal solvents.[63] The preparation of $Zn[C(Me)=CH_2]_2$ (**1**, eq 1) from anhydrous zinc bromide and 2-bromopropene had been reported to proceed in low yield (35%).[64] Combination of 2-bromopropene, lithium metal, and zinc bromide under argon was followed by sonication of the reaction mixture. Removal of diethyl ether under reduced pressure, dissolution into hexanes, filtration, and removal of hexanes gave a pale yellow solid. This solid was sublimed at room temperature under vacuum. Collection of the crystals under a nitrogen atmosphere and resubjecting the remaining solids to sublimation resulted in a combined yield of 66%. Sublimation provided product of high purity as judged by ^1H and $^{13}C\{^1H\}$ NMR spectroscopy (Supporting Information).

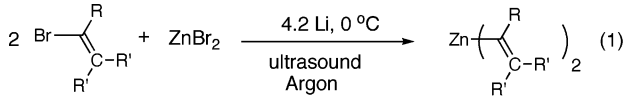

1, R=Me, R'=H, 66% yield
2, R=H, R'=Me, 72% yield

We desired to compare the spectroscopic properties of four-coordinate zinc ligand adducts $L_2Zn[C(Me)=CH_2]_2$ with the parent $Zn[C(Me)=CH_2]_2$ compound. It is known that dialkylzinc complexes of 2,2′-bipyridine (bipy) and diamines, such as tetramethylethylenediamine (tmeda), are four-coordinate and monomeric in the solid state.[65,66] Thus, $Zn[C(Me)=CH_2]_2$ (**1**) was combined with either bipy or tmeda in hexanes (eq 2). Upon addition of bipy to $Zn[C(Me)=CH_2]_2$, a yellow precipitate formed immediately. In contrast, when tmeda was added to $Zn[C(Me)=CH_2]_2$, no precipitate formed and the solution remained clear. The adducts, (bipy)$Zn[C(Me)=CH_2]_2$ (**1•bipy**) and (tmeda)-$Zn[C(Me)=CH_2]_2$ (**1•tmeda**), were isolated in 95 and 90% yield, respectively.

Structures of $Zn[C(Me)=CH_2]_2$ and (bipy)$Zn[C(Me)=CH_2]_2$. Despite the utility of divinylzinc reagents in organic synthesis, we are not aware of any examples of structurally characterized divinylzinc complexes or their derivatives. This may be due to the pyrophoric nature of such compounds. We, therefore, initiated efforts to grow crystals of $Zn[C(Me)=CH_2]_2$ suitable for X-ray analysis. Resublimation of the purified divinylzinc compound **1** under static vacuum for 2 weeks at

(57) Lang, H.; Mansilla, N.; Rheinwald, G. *Organometallics* **2001**, *20*, 1592−1596.
(58) Marek, I.; Beruben, D.; Normant, J.-F. *Tetrahedron Lett.* **1995**, *36*, 3695−3698.
(59) Beruben, D.; Marek, I.; Normant, J. F.; Platzer, N. *J. Org. Chem.* **1995**, *60*, 2488−2501.
(60) Marek, I. *Actual. Chim.* **2003**, *4*−*5*, 17−24.
(61) Lurain, A. E.; Maestri, A.; Kelly, A. R.; Carroll, P. J.; Walsh, P. J. *J. Am. Chem. Soc.* **2004**, *126*, 13608−13609.
(62) Rowley Kelly, A.; Lurain, A. E.; Walsh, P. J. *J. Am. Chem. Soc.* **2005**, *127*, 14668−14674.
(63) Petrier, C.; De Souza Barbosa, J.; Dupuy, C.; Luche, J. L. *J. Org. Chem.* **1985**, *50*, 5761−5765.
(64) Shibata, T.; Nakatsui, K.; Soai, K. *Inorg. Chim. Acta* **1999**, *296*, 33−36.
(65) Charette, A. B.; Molinaro, C.; Brochu, C. *J. Am. Chem. Soc.* **2001**, *123*, 12160−12167.
(66) Mimoun, H.; Yves de Saint Laumer, J.; Giannini, L.; Scopelliti, R.; Floriani, C. *J. Am. Chem. Soc.* **1999**, *121*, 6158−6166.

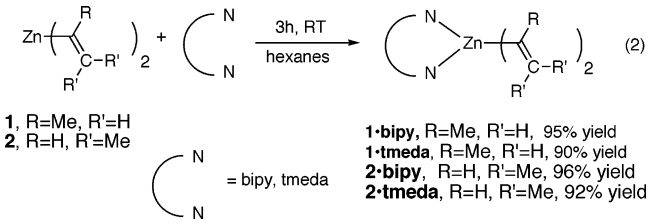

room temperature resulted in formation of long clear needles inside the sublimation apparatus. These crystals were subjected to X-ray crystallographic analysis at low temperature. An ORTEP diagram is illustrated in Figure 4.

Compound **1** consists of an infinite polymeric structure that contains five divinylzinc units in the asymmetric unit cell. The zinc atoms are four-coordinate with a pseudo tetrahedral geometry in which each zinc supports two σ-bonded vinyl groups and two unprecedented π-interactions with the neighboring divinylzinc units. The Zn−C σ-bond distances range from 1.987(9) to 2.006(7) Å, which are comparable to the Zn−C distance of the terminal Zn−Ph bond in the dimer PhZn(μ-Ph)$_2$ZnPh (1.951(5) Å)[67] and close to the distance in the η^1-pentadienyl groups in Zn[CH$_2$=C(*t*Bu)CHC(*t*Bu)=CH$_2$]$_2$ (1.969(8) Å).[68] The olefin C=C distances range from 1.327(10) to 1.359(11) Å, exhibiting little difference from an unbound alkene, a common observation in olefin complexes. The C−Zn−C bond angles between the vinyl σ-bonds in **1** fall between 132.4(3) and 139.4(3)°, indicating a significant deviation from linearity to accommodate the zinc C=C π-interactions (Figures 4 and 5). In contrast, many homoleptic diorganozinc compounds are linear and two-coordinate, akin to simple dialkylzincs.[69] The distances between a zinc and the neighboring C=C bond for C$_\alpha$ range from 2.255(7) to 2.331(8) Å, while the Zn−C$_\beta$ distances fall between 2.267(8) to 2.297(9) Å. These close contacts, together with the C−Zn−C bond angles, clearly indicate the presence of a zinc π-bond. The zinc−π-interactions force the two methyl groups toward one another (Figure 5).

In an effort to disrupt the polymeric nature of **1** in the solid state and to compare relevant bond distances and angles, X-ray quality crystals of **1•bipy** were grown by vapor diffusion of hexanes into a toluene solution containing the compound at room temperature. After several days of diffusion, large yellow crystals were obtained and the structure was determined. An ORTEP diagram is illustrated in Figure 6. The structure of **1•bipy** consists of a monomeric pseudo tetrahedral zinc center. The C=C distances of 1.328(2) Å in **1•bipy** are at the lower end of the range observed for the polymeric parent compound (1.327(10)−1.359(11) Å). The Zn−C distances of 1.998(14) and 2.007(2) Å are unexceptional. The C−Zn−C bond angle of 125.16(6)° is less than the range observed in the polymeric parent compound **1** (132.4(3)−139.4(3)°). The tmeda complex, **1•tmeda**, was a viscous oil in our hands, and attempts to crystallize it were unsuccessful.

Synthesis of Zn[C(H)=CMe$_2$]$_2$ and Derivatives. The unusual π-interaction between zinc and the carbon−carbon double bonds in Zn[C(Me)=CH$_2$]$_2$ inspired us to examine the structure of related divinylzinc complexes. Reaction of 1-bromo-2-methyl-1-propene (eq 1, R = H, R′ = Me) with lithium metal and zinc bromide was performed under conditions similar to those employed for the synthesis of Zn[C(Me)=CH$_2$]$_2$. Sublimation of the crude reaction mixture resulted in isolation of Zn[C(H)=CMe$_2$]$_2$ in 72% yield. X-ray quality crystals of Zn[C(H)=CMe$_2$]$_2$ were grown by sublimation under static vacuum over 4 weeks. For the purpose of comparison, the bipy and tmeda adducts of Zn[C(H)=CMe$_2$]$_2$ were synthesized by mixing complex **2** with each bidentate ligand (eq 2). When bipy was added to a hexanes solution of Zn[C(H)=CMe$_2$]$_2$, a yellow precipitate formed immediately. In contrast, no precipitate formed and the solution remained clear when tmeda was mixed with **2**. The adducts, (bipy)Zn[C(H)=CMe$_2$]$_2$ (**2•bipy**) and (tmeda)Zn[C(H)=CMe$_2$]$_2$ (**2•tmeda**) were isolated in 96 and 92% yield, respectively.

Structures of Zn[C(H)=CMe$_2$]$_2$, (bipy)Zn[C(H)=CMe$_2$]$_2$, and (tmeda)Zn[C(H)=CMe$_2$]$_2$. The structure of Zn[C(H)=CMe$_2$]$_2$ (**2**) was determined by X-ray crystallography and is illustrated in Figure 7. In the solid state, the structure of **2** consists of an extended network of zinc atoms forming a polymeric architecture. Each zinc atom in **2** is pseudo tetrahedral with four bridging σ-bonded vinyl groups (Figure 8).

The Zn−C bond lengths in **2** range from 2.003(11) to 2.346(10) Å, close to the range found in dimeric PhZn(μ-Ph)$_2$ZnPh [1.951(5) (terminal) and 2.006(5)−2.442(4) Å (bridging)].[67] The C=C bond lengths in **2** range from 1.312(14) to 1.380(14) Å. The vinyl bridges hold the zinc centers in close contact, with the interatomic distances ranging from 2.512(2) to 2.587(2) Å (cf. 2.669(4) Å for metallic zinc).[25] The Zn−C−Zn angles inside the central rings are small with angles ranging from 71.0(3) to 74.0(3)°, whereas the C−Zn−C angles are larger ranging from 101.9(4) to 105.8(4)°.

For the purpose of comparison, yellow crystals of **2•bipy** were grown by vapor diffusion using a hexanes/toluene combination. An ORTEP diagram of this compound is illustrated in Figure 9. Additionally, **2•tmeda** was crystallized via slow evaporation of a hexanes solution at room temperature under nitrogen. The ORTEP diagram of **2•tmeda** is shown in Figure 10.

In contrast to polymeric parent Zn[C(H)=CMe$_2$]$_2$ (**2**), **2•bipy** and **2•tmeda** are monomeric in the solid state. The metrical parameters for both compounds are similar and are only briefly outlined. Interestingly, the respective C−Zn−C bond angles of **2•bipy** and **2•tmeda** are 138.88(8) and 144.47(8)°. These angles are considerably larger than the idealized tetrahedral bond angles and are similar to those observed in polymeric Zn[C(Me)=CH$_2$]$_2$ (**1**, 132.4(3)−139.4(3)°). The C=C distances of **2•bipy** and **2•tmeda** are 1.336(3) and 1.324(3) Å and fall within the range of those observed in the polymeric Zn[CH=CMe$_2$]$_2$ [1.312(14) to 1.380(14) Å]. The Zn−C$_\alpha$ bond distances for **2•bipy** are 1.979(2) and 1.992(2) Å, which are similar to those of **2•tmeda** of 1.982(2) and 1.989(2) Å.

Solution and Solid-State NMR and IR Studies of the Divinylzinc Complexes. Given the interesting and unexpected solid-state structures of **1** and **2**, we desired to explore their solution phase characteristics. Polymeric divinylzinc compounds **1** and **2** readily dissolved in benzene-d_6, and their NMR spectra were recorded. Given the sensitivity of chemical shifts in the ^{13}C{^{1}H} NMR to local environments, we decided to investigate and compare the solution and solid-state ^{13}C{^{1}H} NMR spectra

(67) Markies, P. R.; Schat, G.; Akkerman, O. S.; Bickelhaupt, F.; Smeets, W. J. J.; Spek, A. L. *Organometallics* **1990**, *9*, 2243−2247.
(68) Ernst, R. D.; Freeman, J. W.; Swepston, P. N. *J. Organomet. Chem.* **1991**, *402*, 17−25.
(69) Almenningen, A.; Helgaker, T. U.; Haaland, A.; Samdal, S. *Acta Chem. Scand. Ser. A: Phys. Inorg. Chem.* **1982**, *36*, 159−166.

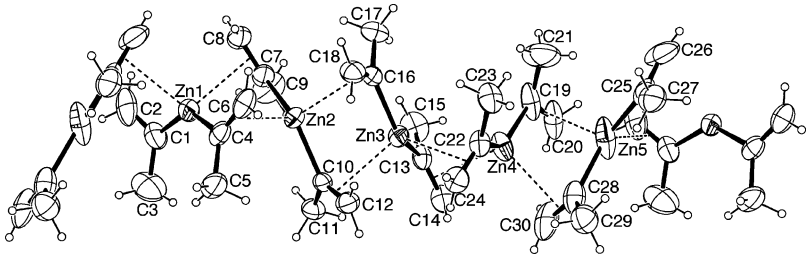

Figure 4. View of the five divinylzinc molecules in the asymmetric unit cell of **1** with 30% probability thermal ellipsoids.

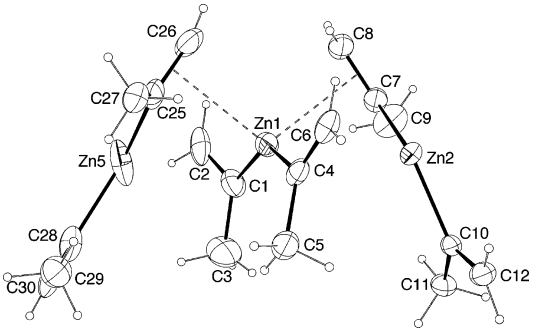

Figure 5. View of the divinylzinc unit in **1** with 30% probability thermal ellipsoids.

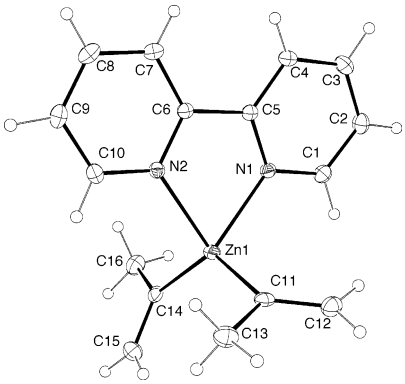

Figure 6. ORTEP diagram of (bipy)Zn[C(Me)═CH_2]$_2$ (**1•bipy**) with 30% probability thermal ellipsoids.

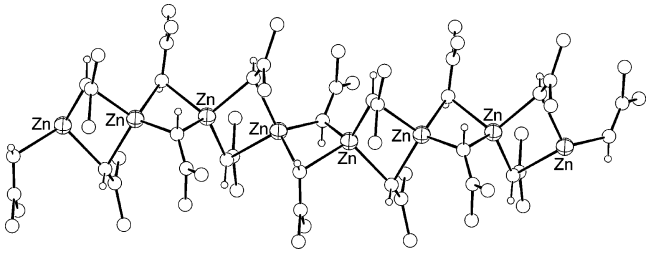

Figure 7. ORTEP drawing of the polymer chain formed in subunit no. 1 of complex **2**.

of **1** to monomeric **1•bipy** and **1•tmeda**. The solution and solid-state $^{13}C\{^1H\}$ NMR chemical shifts of **1**, **1•bipy**, and **1•tmeda** are tabulated in Table 1.

The $^{13}C\{^1H\}$ NMR resonances of Zn(C(Me)═CH_2)$_2$ (**1**), **1•bipy**, and **1•tmeda** in C_6D_6 are listed in Table 1. The chemical shift differences, $\Delta\delta$, observed in solution and the solid state for the α- and β-carbons of Zn(C(Me)═CH_2)$_2$ (**1**) were 6.3 and 3.1 ppm, respectively. The $^{13}C\{^1H\}$ NMR spectra of Zn(C(Me)═CH_2)$_2$ were recorded at different concentrations in C_6D_6. Over a 10-fold concentration range of **1** (0.12−1.2 M), the chemical shifts of the α- and the β-carbons exhibited only small differences (0.8 ppm for C_α and 0.1 ppm for C_β), suggesting that no significant change in aggregation state occurred over this concentration range. Solution chemical shift differences between **1** and **1•bipy** of 3.3 and 5.6 ppm were

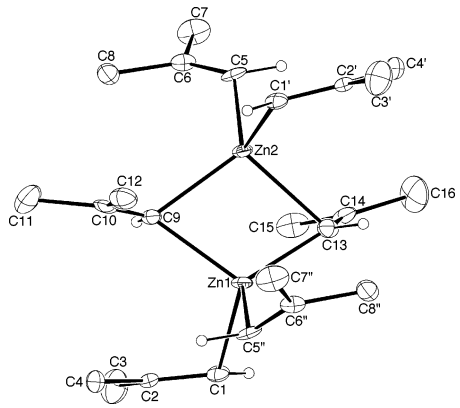

Figure 8. ORTEP drawing illustrating the bridging interactions in **2**.

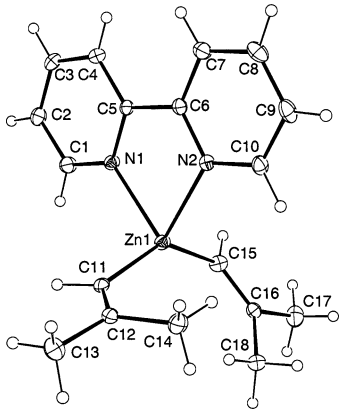

Figure 9. ORTEP diagram of (bipy)Zn[C(H)═CMe_2]$_2$ (**2•bipy**) with 30% probability thermal ellipsoids.

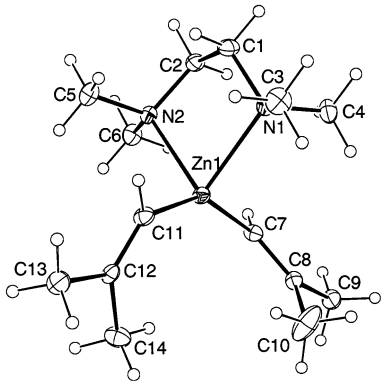

Figure 10. ORTEP diagram of (tmeda)Zn[C(H)═CMe_2]$_2$ (**2•tmeda**) with 30% probability thermal ellipsoids.

Table 1. $^{13}C\{^1H\}$ NMR Chemical Shifts of the Vinyl Groups in **1**, **1•bipy**, and **1•tmeda** in the Solid State (in parentheses) and in C_6D_6 (ppm)

compound	C_α	C_β	Me
$Zn[C(Me)=CH_2]_2$	(173.4)[a]	(124.2)[a]	(32.6)[a]
	167.1	127.3	30.4
$(bipy)Zn[C(Me)=CH_2]_2$	170.4	121.7	32.2
$(tmeda)Zn[C(Me)=CH_2]_2$	169.0	122.8	33.5

[a] Solid-state $^{13}C\{^1H\}$ chemical shifts.

Table 2. $^{13}C\{^1H\}$ NMR Chemical Shifts of **2**, **2•bipy**, and **2•tmeda** of the Vinyl Groups in the Solid State (in parentheses) and in C_6D_6 (ppm)

compound	C_α	C_β	Me	Me
$(Zn[C(H)=CMe_2]_2$	(130.0)[a]	(172.4)[a]	(33.0)[a]	(30.1)[a]
	134.6	156.7	30.0	29.8
$(bipy)Zn[C(H)=CMe_2]_2$	145.7	144.8	30.9	29.0
$(tmeda)Zn[C(H)=CMe_2]_2$	143.4	145.4	31.0	29.1

[a] Solid-state $^{13}C\{^1H\}$ chemical shifts.

observed for C_α and C_β, respectively. Similarly, **1** and **1•tmeda** gave solution chemical shift differences of 1.9 (C_α) and 4.5 ppm (C_β). The $\Delta\delta$ values between **1** and **1•bipy** and **1** and **1•tmeda** are smaller than those observed between **1** in solution and solid state.

The solution IR spectra of **1**, **1•tmeda**, and **1•bipy** in CH_2Cl_2 exhibited C=C vibrations at 1560 cm^{-1} for **1** and 1568 cm^{-1} for **1•tmeda**. The IR of **1•bipy** was more complicated due to the overlap of the aromatic C−C absorptions of the bipy ligand with the vinyl group. Absorbances for **1•bipy** were observed at 1594, 1572, and 1565 cm^{-1}. The solid-state IR of **1** exhibited a C=C absorption at 1560 cm^{-1}. Absorptions for the vinyl groups are all blue shifted compared to the C=C absorptions for the starting alkenylbromide (1648 cm^{-1}).

In a study of the related $ZnPh_2$, it was found that the solid-state structure is a dimer with bridging phenyl groups, PhZn-(μ-Ph)$_2$ZnPh. Solution studies, however, were consistent with a monomeric two-coordinate complex.[67] Although the solution spectroscopic data outlined above do not allow definitive assignment of the solution-state structure, it is likely that **1** is monomeric in solution.

NMR data for **2** are listed in Table 2. Compound **2** exhibits $\Delta\delta$ values for C_α and C_β between the solution and solid state of 4.6 and 15.7 ppm, respectively, suggesting a change in bonding between solution and solid state. Examination of the chemical shift differences of **2** in C_6D_6 over a 10-fold concentration range (0.1−1.0 M) exhibited no change in the position of the C_α resonance and a deviation of 2 ppm in the C_β resonance. These data suggest that there is no change in the state of aggregation over this concentration range. When the solution $^{13}C\{^1H\}$ NMR of **2** was compared to that of **2•bipy**, $\Delta\delta$ values of 11.1 (C_α) and 11.9 ppm (C_β) were measured. Likewise, **2** and **2•tmeda** exhibited $\Delta\delta$ values of 8.8 (C_α) and 11.3 ppm (C_β) (Table 2). Determination of the solution molecular weight by the Signer method[70] using ferrocene as a standard was most consistent with **2** existing as a monomer in solution.

Solution IR spectra were obtained in CH_2Cl_2 for **2**, **2•tmeda**, and **2•bipy**. Compound **2** exhibited a C=C absorbance at 1565 cm^{-1}, while a C=C absorbance at 1587 cm^{-1} was observed for **2•tmeda**, and three C=C absorbances at 1594, 1586, and 1562 cm^{-1} were observed for **2•bipy**, of which 1586 cm^{-1} was assigned to the vinyl group by comparison to **1•bipy**. The solution NMR studies provide little insight into the solution structure of **2**.

(70) Zoellner, R. W. *J. Chem. Educ.* **1990**, *67*, 714−715.

Conclusions

Herein, we disclose novel solid-state structures of two homoleptic divinylzinc complexes, $Zn[C(Me)=CH_2]_2$ (**1**) and $Zn[C(H)=CMe_2]_2$ (**2**). Both structures consist of infinite polymeric chains, although the nature of the bridging groups is completely different. The solid-state structure of $Zn[C(H)=CMe_2]_2$ consists of bridging vinyl groups in which the α-carbons of the vinyl groups each bridge two zinc centers. In the solid-state structure of $Zn[C(Me)=CH_2]_2$, the divinylzinc units are held together by unprecedented Zn−π-interactions. The Zn−C distances to the neighboring π-bonds are quite short, ranging from 2.255(7) to 2.331(8) Å. These bond lengths can be compared to the Zn−C σ-bond lengths of 1.987(9)−2.006(7) Å. $Zn[C(Me)=CH_2]_2$ represents the first structurally characterized zinc−olefin complex. Analysis of solid-state and solution NMR studies suggests that the Zn···C π-bond does not greatly perturb the electronic environment around the C=C bond. On the basis of the results of our studies, we hypothesize that the zinc−π-interactions do not persist in solution. The different bonding in the vinyl groups of these divinylzinc complexes is likely due to the different degree of steric hindrance about the α-carbon. In $Zn[C(H)=CMe_2]_2$, the α-carbons are unhindered and readily form σ-bridges. In contrast, the α-methyl groups of $Zn[C(Me)=CH_2]_2$ hinder bridging through σ-interactions, resulting in formation of π-bonds.

Although Zn(II) has the same d^{10} electronic configuration as Ni(0), Pd(0), and Pt(0), which are well-known to bind olefins, the high promotional energy of Zn(II) indicates that zinc will exhibit little or no back-bonding. This study provides the first direct evidence for zinc(II)−π-interactions with uncharged π-systems. Previously, the interaction of zinc(II) with olefins had been invoked to explain stereocontrol in diastereoselective reactions. Prior investigations into zinc−olefin π-interactions, however, concluded that these interactions were weak and that the zinc−olefin distance was long (3.0 Å), increasing the speculative nature that such interactions could significantly impact reaction outcomes. The structure of $Zn[C(Me)=CH_2]_2$ demonstrates that zinc can indeed form olefin complexes, lending credence to the proposal that such interactions can play a significant role in governing stereochemistry.

Experimental Section

General Methods: All reactions and manipulations were carried out under an inert atmosphere in a Vacuum Atmospheres drybox with attached MO-40 Dritrain, or by using standard Schlenk or vacuum line techniques with oven-dried glassware. The ultrasound reactions were run under a strong flow of argon gas that was dried via passage through drierite and a copper catalyst. The progress of all reactions was monitored by the consumption of lithium metal and by the generation of a deep black colored solution that developed over ca. 1 h. Dichloromethane, toluene, and hexanes (UV grade, alkene-free) were dried through alumina columns under nitrogen. Diethyl ether and tetrahydrofuran were predried through alumina columns and further dried using sodium/benzophenone ketyl. Pentane (HPLC grade) was dried using sodium/benzophenone ketyl. Solutions were degassed as follows: they were cooled to −196 °C, evacuated under high vacuum,

and thawed. This sequence was repeated three times in each case. Unless otherwise specified, all reagents were purchased from Aldrich Chemical Co., Acros, or Strem Chemicals, and all solvents were purchased from Fischer Scientific. Deuterated solvents were purchased from Cambridge Isotopes. THF-d_8 was vacuum transferred from sodium/benzophenone ketyl. Tetramethylethylenediamine (TMEDA) was dried from KOH, heated on an oil bath, and collected via fractional distillation under nitrogen. The ^{1}H and ^{13}C{^{1}H} NMR spectra were obtained on a Bruker DMX-300 or on a Bruker AM-500 Fourier transform NMR spectrometer at 300 and 75 MHz or 500 and 125 MHz, respectively. Chemical shifts are recorded in units of parts per million downfield from tetramethylsilane and are reported relative to the deuterated solvent residual proton resonance. All coupling constants are reported in Hertz. The infrared spectra were obtained using a Perkin-Elmer 1600 series spectrometer. The synthesis of **1** has been described previously.[55,56]

Synthesis of Zn[C(Me)═CH$_2$]$_2$ (1): A 250 mL Schlenk flask was charged with $ZnBr_2$ (12.05 g, 53.5 mmol) and a magnetic stir bar. The flask was heated in an oil bath at 130 °C in vacuo (0.2 mmHg) for 3.5 h and then cooled to room temperature. Lithium wire (1.57 g, 226 mmol) was quickly cut into small pieces in mineral oil and then washed with 3 × 10 mL dry hexanes under a steady flow of argon. The Schlenk flask was charged with the lithium metal followed by addition of diethyl ether (90 mL). The solution was placed in the center of the ultrasound unit filled with ice water, and then 2-bromopropene (9.75 mL, 110 mmol) was injected into the flask. The flask was sonicated for 1.5−2 h until the lithium was consumed and a black color developed after 30 min of reaction time. The solvent was almost completely removed under reduced pressure; 30 mL of hexanes was added and the solution allowed to stand for 30 min. In a nitrogen-filled drybox, the dark, grayish solids were filtered through Celite and washed with 2 × 30 mL of hexanes. The pale yellow solution was poured into a Schlenk flask. The solvent was then removed under reduced pressure, and a pale yellow solid precipitated from the solution as the flask cooled. After drying for 30 min in vacuo, a coldfinger was inserted into the Schlenk flask and the yellow solid was sublimed at room temperature (0.2 mmHg). The sublimed material was collected from the coldfinger, and the remaining solid again was subjected to sublimation. This process was repeated two more times, producing in total 5.22 g of a white solid (66% yield based on 2-bromopropene). ^{1}H NMR (C_6D_6, 300 MHz): δ 1.97 (t, 3H, J = 1.50 Hz, CH_3), 5.33 (m, 1H, J = 1.38 Hz, Zn[MeC═CHH]$_2$), and 5.88 (m, 1H, J = 1.60 Hz, Zn[MeC═CHH]$_2$) ppm. ^{13}C{^{1}H} NMR (C_6D_6, 75 MHz): δ 30.4, 127.3, and 167.1 ppm. IR {KBr and CH_2Cl_2}: ν 300.7 (s), 2919 (s), 2900 (s), 2837 (s), 1560 (s), 1443 (s), 1428 (s), 1362 (s), 1024 (w), 996 (w), 928 (s), 915 (s), 522 (w) cm^{-1}; melting range 65−70 °C.

Synthesis of Zn[C(H)═CMe$_2$]$_2$ (2): The compound was prepared according to the procedure for **1** using $ZnBr_2$ (10.98 g, 48.8 mmol), lithium wire (1.42 g, 205 mmol), 1-bromo-2-methylpropene (13.18 g, 97.6 mmol), and diethyl ether (90 mL). Divinyl complex **2** was sublimed at room temperature three consecutive times, producing 6.15 g in total of a white solid (72% based on 1-bromo-2-methylpropene). ^{1}H NMR (C_6D_6, 300 MHz): δ 1.85 (s, 3H, CH_3), 1.95 (d, 3H, J = 1.20 Hz, CH_3), and 5.52 (br s, 1H, Zn, HC═CMe$_2$) ppm. ^{13}C{^{1}H} NMR (C_6D_6, 75 MHz): δ 29.81, 29.95, 134.6, and 156.7 ppm. IR {CH_2Cl_2 and KBr}: ν 2970 (s), 2919 (s), 2899 (s), 2840 (s), 1565 (s), 1430 (s), 1362 (s), 1123 (m), 991 (m), 827 (s), 608 (m), 587 (m) cm^{-1}; melting range 63−67 °C.

Synthesis of 1•bipy: Under a glovebox atmosphere, bipy (0.318 g, 2.03 mmol) was dissolved in 20 mL of hexanes and added slowly to a 20 mL hexanes solution of compound **1** (0.300 g, 2.03 mmol). Upon mixing, a yellow precipitate was produced immediately. After stirring this solution at room temperature for 3 h, the yellow solid was collected via vacuum filtration and washed once with 5 mL of hexane. This solid was dried in vacuo, and 0.587 g of the desired compound was obtained (95% yield based on Zn[C(Me)═CH$_2$]$_2$. X-ray quality crystals can be obtained via vapor diffusion of pentane into a toluene solution of **1•bipy**. ^{1}H NMR (C_6D_6, 300 MHz): δ 2.29 (t, 3H, J = 1.5 Hz, CH_3), 5.47 (dq, 1H, J = 5.9, 1.4 Hz, (bipy)Zn[MeC═CHH]$_2$), 6.21 (dq, 1H, J = 5.9, 1.6 Hz, (bipy)Zn[MeC═CHH]$_2$), 6.51 (qd, 1H, J = 7.5, 5.0, 1.4, 1.1 Hz, bipy), 7.02 (td, 1H, J = 15.6, 7.6, 1.7 Hz, bipy), 7.16 (t, 1H, J = 8.1 Hz, bipy), and 8.24 (dq, 1H, J = 5.0, 2.4 Hz, bipy) ppm. ^{13}C{^{1}H} NMR (C_6D_6, 75 MHz): δ 32.2, 121.4, 121.7, 125.4, 138.5, 148.8, 151.4, and 170.4 ppm. IR {KBr and CH_2Cl_2}: ν 3064 (m), 2985 (s), 2913 (s), 2881 (s), 2825 (s), 1594 (s), 1572 (s), 1565 (s), 1488 (s), 1474 (s), 1440 (s), 1312 (m), 1246 (w), 1165 (m), 1152 (m), 1099 (w), 1015 (s), 999 (m), 927 (m), 881 (s), 872 (s), 764 (s), 737 (s), 645 (m), 528 (m) cm^{-1}; melting range 95−100 °C.

Synthesis of 2•bipy: Under a glovebox atmosphere, bipy (0.267 g, 1.71 mmol) was dissolved in 20 mL of hexanes and added slowly to a 20 mL hexanes solution of compound **2** (0.300 g, 1.71 mmol). Upon mixing, a yellow precipitate was produced immediately. After stirring this solution at room temperature for 3 h, the yellow solid was collected via vacuum filtration and washed once with 5 mL of hexane. This solid was dried in vacuo, and 0.545 g of the desired compound was obtained (96% yield based on Zn[C(H)═CMe$_2$]$_2$). Orange X-ray quality crystals can be obtained via vapor diffusion of pentane into a toluene solution of **2•bipy**. ^{1}H NMR (C_6D_6, 300 MHz): δ 2.27 (d, 3H, J = 1.1 Hz, CH_3), 2.40 (s, 3H, CH_3), 6.18 (br s, 1H, (bipy)Zn[HC═CMe$_2$]$_2$), 6.53 (br s, 1H, bipy), 6.96 (br t, 1H, J = 7.3 Hz, bipy), 7.19 (br d, 1H, J = 4.1 Hz, bipy), and 8.43 (dq, 1H, J = 5.0, 0.68 Hz, bipy) ppm. ^{13}C{^{1}H} NMR (C_6D_6, 75 MHz): δ 29.0, 30.9, 121.2, 125.0, 138.0, 144.8, 145.6, 149.1, and 151.6 ppm. IR {KBr and CH_2Cl_2}: ν 3066 (m), 2960 (s), 2884 (s), 2835 (s), 1594 (s), 1586 (s), 1562 (s), 1471 (s), 1438 (s), 1357 (m), 1312 (m), 1247 (w), 1155 (w), 1109 (m), 1060 (w), 1015 (w), 825 (s), 806 (s), 756 (s), 736 (s), 643 (m), 622 (s), 607 (s) cm^{-1}; melting range 130−135 °C. Anal. Calcd for $C_{18}H_{22}N_2Zn$: C, 65.17; H, 6.68; N, 8.44. Found: C, 64.89; H, 6.54; N, 8.48.

Synthesis of 1•tmeda: Under a glovebox atmosphere, tmeda (0.307 mL, 0.236 g, 2.03 mmol) was added to a 40 mL hexanes solution of compound **1** (0.300 g, 2.03 mmol). Upon mixing, the solution remained clear and was stirred at room temperature for an additional 3 h. All volatile materials were removed in vacuo, and a clear viscous liquid was obtained. After complete drying, 0.481 g of the desired compound was obtained as an oil (90% yield based on Zn[C(Me)═CH$_2$]$_2$. ^{1}H NMR (C_6D_6, 300 MHz): δ 1.93 (s, 2H, Me$_2$NC$_2$$H_4NMe_2$), 2.03 (s, 6H, Me_2-NC$_2H_4NMe_2$), 2.18 (t, 3H, J = 1.5 Hz, (tmeda)Zn[MeC═CHH]$_2$), 5.17 (dq, 1H, J = 5.7, 1.3 Hz, (tmeda)Zn[MeC═CHH]$_2$), and 5.97 (dq, 1H, J = 5.7, 1.6 Hz, (tmeda)Zn[MeC═CHH]$_2$) ppm. ^{13}C{^{1}H} NMR (C_6D_6, 75 MHz): δ 33.5, 47.9, 57.7, 122.8, and 169.0 ppm. IR {KBr and CH_2Cl_2}: ν 3126 (s), 2999 (s), 2964 (s), 2885 (s), 1568 (m), 1461 (s), 1354 (s), 1289 (s), 1250 (s), 1184 (m), 1162 (s), 1127 (s), 1100 (m), 1063 (s), 1031 (s), 1015 (s), 951 (s), 932 (s), 919 (s), 887 (s), 794 (s), 771 (s), 680 (s), 739 (w), 583 (s), 527 (s), 472 (s) cm^{-1}.

Synthesis of 2•tmeda: Under a glovebox atmosphere, tmeda (0.258 mL, 0.199 g, 1.71 mmol) was added to a 40 mL hexanes solution of compound **2** (0.300 g, 1.71 mmol). Upon mixing, the solution remained clear and was stirred at room temperature for an additional 3 h. All volatile materials were removed in vacuo, and a white solid was obtained. After complete drying, 0.459 g of the desired compound was obtained (92% yield based on Zn[C(H)═CMe$_2$]$_2$). X-ray quality crystals can be obtained via slow evaporation of a hexanes solution of **2•tmeda**. ^{1}H NMR (C_6D_6, 300 MHz): δ 1.74 (s, 2H, Me$_2$NC$_2$$H_4NMe_2$), 1.95 (s, 6H, Me_2NC$_2H_4$NMe_2), 2.24 (s, 3H, (tmeda)Zn[HC═CMeMe]$_2$), 2.28 (d, 3H, J = 1.1 Hz, (tmeda)Zn[HC═CMeMe]$_2$), and 5.88 (br q, 1H, J = 0.56 Hz, (tmeda)Zn[HC═CMeMe]$_2$) ppm. ^{13}C{^{1}H} NMR (C_6D_6, 75 MHz): δ 29.1, 31.0, 47.2, 57.2, 143.4, and 145.4 ppm. IR {KBr and CH_2Cl_2}: ν 3002 (s), 2955 (s), 2885 (s), 2845 (s), 1587 (s), 1456 (s), 1434 (s), 1358 (s), 1288 (s), 1267 (m), 1253 (m), 1182 (m), 1158 (m), 1125 (s), 1114 (s), 1064 (s), 1033 (s), 1018 (s), 950 (s), 937 (m), 808 (s) 791 (s), 770 (s), 739 (s), 621 (s), 582 (w) cm^{-1}; melting range 79−83 °C. Anal. Calcd for: C 57.63% H 10.36% N 9.60%; Found: C 57.39% H 10.12% N 9.54%.

Acknowledgment. We are grateful to Dr. Walter Boyko and Professor Brian Ohta (Villanova University) for obtaining solid-state NMR spectra of compounds **1** and **2**. We thank Professors Larry G. Sneddon and Don Berry for helpful discussions. This work was supported by the National Science Foundation (CHE-0315913) and the National Institutes of Health (GM58101).

Supporting Information Available: Procedures and full characterization of new compounds (PDF) and the CIF files for compounds **1** and **2** are available. This material is available free of charge via the Internet at http://pubs.acs.org.

JA058700X